Original scientific paper

HBEM ANALYSIS OF ELLIPTICAL-SHAPED MICROSHIELD LINES: PARAMETER EFFECTS AND SIMULATION VALIDATION

Mirjana Perić, Natalija Ivković, Isidora Jovanović

University of Niš, Faculty of Electronic Engineering, Niš, Serbia

ORCID iDs:		
	Mirjana Perić	ⓘ https://orcid.org/0000-0001-8670-2254
	Natalija Ivković	ⓘ https://orcid.org/0009-0006-5218-4544
	Isidora Jovanović	ⓘ https://orcid.org/0009-0000-1150-6611

Abstract. *This paper employs the hybrid boundary element method to ascertain the characteristic parameters of elliptic-shaped microshield lines. As a special case of these lines, the microshield with circular shape is also analysed. The study investigates the impact of various parameters on the characteristic impedance as well as effective relative permittivity. A comparison is made between the results obtained from the proposed method and those acquired through simulation software, revealing a high level of agreement.*

Key words: *Characteristic parameters, finite element method, hybrid boundary element method, microshield lines*

1. INTRODUCTION

Microshield lines can be considered as an evolution part of conventional microstrip lines, as they avoid some of the technology problems that appear in classical microstrip lines. These lines can operate without the need for via holes or the use of air bridges for ground equalization, which can be sources of signal loss and noise. Also, the shield helps to reduce electromagnetic coupling between adjacent lines.

In [2], the edge-based finite element method is applied to analyse trapezoidal shaped microshield lines, considering configurations with one, two and three strips. The paper undertakes a full-wave analysis, determining cut-off wavelengths and field patterns for various geometries and conductors' positions. Kiang [3] employs a potential-matching approach to calculate the capacitance as well as characteristic impedance of microshield lines with trapezoidal, circular and V-shaped shields and layered substrates. This study encompasses lower shielded and fully shielded lines, highlighting the impact of the conductors and gap widths on characteristic parameters. The author emphasizes the

significance of coplanar and shield ground positions in influencing field distribution and thus determines the trend of the characteristic impedance variation. Characteristic impedance's analytical expressions for V, elliptic and circular-shaped microshield lines are established in [4] through the conformal mapping method, presuming pure-TEM propagation. The authors adopt a graphical approximation, particularly suitable for circular and elliptic-shaped lines, along with the estimation method. This estimation method finds application in calculating the characteristic impedance of coaxial lines with square and rectangular inner conductors. Following this approach, the characteristic impedance is determined as the mean value between upper and lower bounds. The effects of different microshield shapes are presented through the obtained numerical results. Dib and Katehi applied in [5] the conformal mapping method along with the point matching method, for rectangular-shaped single microshield lines analysis. Open sided single and coupled microshield structures are assumed for simplicity in [6], where the conformal mapping method is also used. The coupling coefficient distribution is determined. As a type of machine learning process, an artificial neural network has been applied in [7] for characteristic parameters determination of elliptic and circular-shaped microshield lines. Several algorithms have been used to train the neural models. Training data sets are obtained following the procedure given in [4]. The authors concluded that the obtained results are in close match with the results that can be found in the literature.

It is also possible to use the hybrid boundary element method (HBEM) for the microshield lines analysis. The quasi-static TEM analysis of V-shaped microshield lines is performed in [8] to determine the characteristic parameters for single as well as coupled structures.

Based on the HBEM application for the microstrip lines analysis, the characteristic parameters of single and coupled elliptic-shaped microshield lines will be calculated in this paper. The code, written in [8], had to be modified, considering that different configurations should be analysed. The effects of the parameters and dimensions of elliptic-shaped microshield lines on the characteristic impedance and effective relative permittivity will be shown. Those geometries are presented in Fig. 1.

The conductors, of width w and thickness d, are placed on a substrate of elliptical cross-section, with the relative permittivity ε_r, width b and thickness h_2. The slot width is denoted with s. A circular shaped microshield line is the special form of the elliptic-shaped geometry when h_2 and $b/2$ are equal. The upper part of the shield is of width a and height h_1.
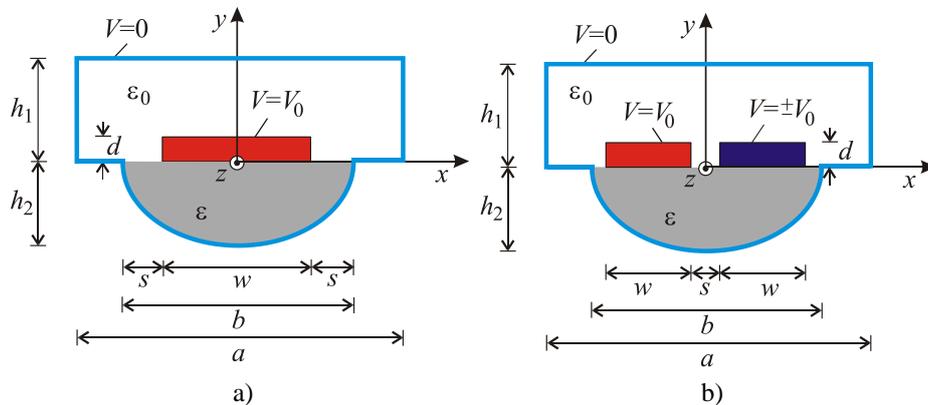

Fig. 1 (a) Single elliptic-shaped microshield line; (b) Coupled elliptic-shaped microshield line

In the case of the single microshield line, Fig. 1a, the strip is on the potential $V = V_0$. When the coupled structure is analysed, Fig. 1b, the both strips are on the potential V_0 (even mode) or on the opposite potentials $\pm V_0$ (odd mode). The shield is on the zero potential ($V = 0$) for both geometries.

The paper begins with a brief theoretical background on the hybrid boundary element method. Following this, numerical results for characteristic parameters are provided for structures, both single and coupled, with elliptical and circular cross-sections. The modelling of these geometries was carried out using the FEMM software [9], and the obtained results were subsequently verified against the HBEM values.

The obtained results have been discussed. Main conclusions are given in the last section of this paper.

2. THEORETICAL BACKGROUND

For over a decade, the hybrid boundary element method has demonstrated its successful utilization in solving various electromagnetic problems. In-depth elucidation of its application in microstrip line analysis can be found in [10-13].

This method offers versatility in tackling both two and three-dimensional problems. Its simplicity and precision set it apart from alternative approaches, presenting a fusion of the equivalent element method (EEM), the boundary element method (BEM) and the point matching of the electric scalar potential and electric field strength vector components.

Main part of this method is an introduction of the equivalent electrodes concept, taken from the EEM. Nevertheless, the EEM falls short when handling heterogeneous media, unlike HBEM.

In the HBEM approach, all boundaries within the designated geometry are portioned into strips, each of which is substituted with the equivalent electrodes (EEs). In order to illustrate this concept, in Fig. 2a a multilayered coupled microshield line with arbitrary shield as well as arbitrary strips cross-sections is presented.

The corresponding HBEM model is given in Fig. 2b. At the separating surfaces of two layers the polarized charges are placed in the air. Free charges are placed in corresponding dielectric at the conductors' surfaces. Although the total (free and polarized) charges actually exist at the conductors' surfaces, it is shown in [10] that an approximation with acceptable accuracy can be done; therefore, only the free charges are taken into account.

Using that approximation, the electric scalar potential at any point of the formed equivalent electrodes system from the Fig. 2b is

$$
\begin{aligned}
V = A &- \sum_{k=1}^{K_1} \frac{q'_{\text{f}1k}}{2\pi\varepsilon_{i+1}} \ln \sqrt{(x - x_{\text{f}1k})^2 + (y - y_{\text{f}1k})^2} - \\
&- \sum_{k=1}^{K_2} \frac{q'_{\text{f}2k}}{2\pi\varepsilon_i} \ln \sqrt{(x - x_{\text{f}2k})^2 + (y - y_{\text{f}2k})^2} - \\
&- \sum_{k=1}^{K_3} \frac{q'_{\text{f}3k}}{2\pi\varepsilon_{corresponding\,layer}} \ln \sqrt{(x - x_{\text{f}3k})^2 + (y - y_{\text{f}3k})^2} - \\
&- \sum_{j=1}^{N-1} \sum_{m=1}^{M_j} \frac{q'_{\text{p}jm}}{2\pi\varepsilon_0} \ln \sqrt{(x - x_{\text{p}jm})^2 + (y - y_{\text{p}jm})^2} ,
\end{aligned}
\tag{1}
$$

where M_j - is the number of equivalent electrodes (EEs) (polarized charges) on the j-th boundary surface between two layers ($j = 1,\ldots, (N-1)$), K_i ($i = 1, 2, 3$) - is the number of equivalent electrodes (EEs) (free charges) on the boundary surface between the conductor and the layer, and A is an additional constant. q'_f and q'_p are free and polarized line charges (equivalent electrodes), respectively. With (x_f, y_f) and (x_p, y_p) the positions of those charges are denoted
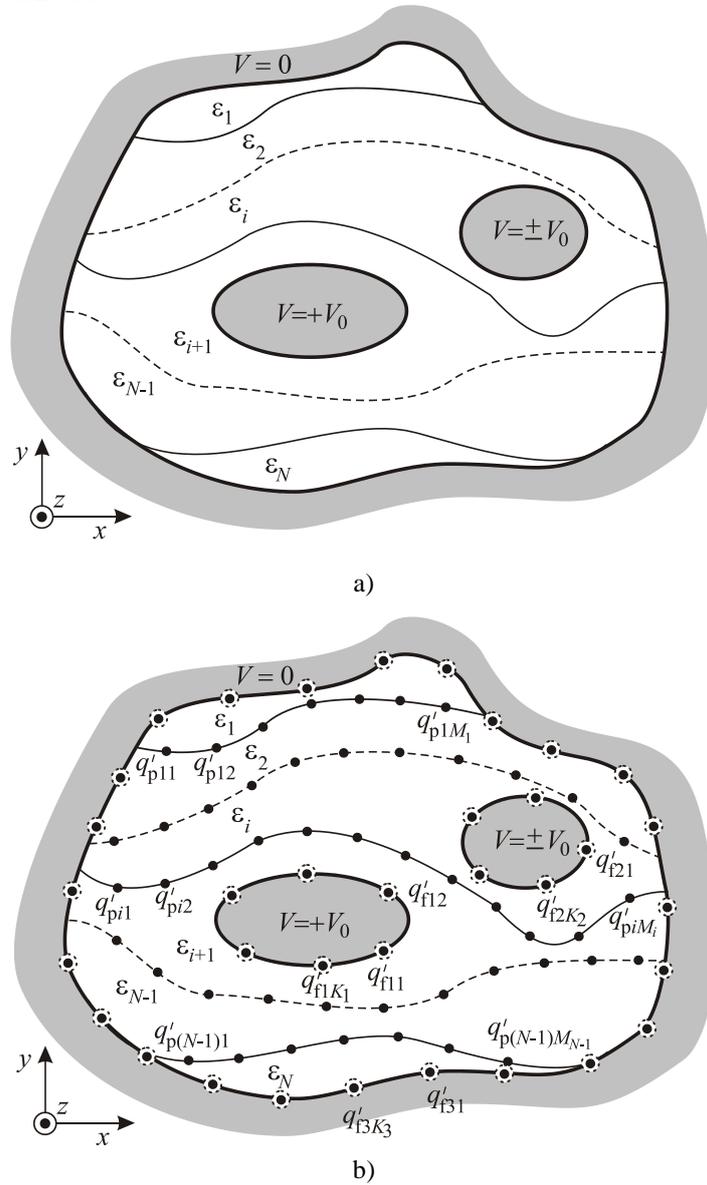

a)

b)

Fig. 2 a) Multilayered coupled microshield line; b) HBEM model

The electric field strength vector is

$$\boldsymbol{E} = -\operatorname{grad} V . \tag{2}$$

The total number of unknowns (equivalent electrodes), N_{tot}, is denoted by:

$$N_{\text{tot}} = \sum_{i=1}^{3} K_i + \sum_{j=1}^{N-1} M_j + 1 . $$

At the interfaces of two layers, the boundary condition is employed to govern the normal component of electric field strength vector. Moreover, the potential along the created model aligns with the strips and shield potentials. This process culminates in the formulation of a system of linear equations. Solving this system yields the values of equivalent electrodes charges, enabling the calculation of the system's capacitance, characteristic impedance, effective relative permittivity, and more.

The effective permittivity and characteristic impedance of the elliptic-shaped microshield line are given as

$$\varepsilon_{\text{r}}^{\text{eff}} = \frac{C'}{C'_0} \quad \text{and} \tag{3}$$

$$Z_{\text{c}} = \frac{Z_{\text{c}0}}{\sqrt{\varepsilon_{\text{r}}^{\text{eff}}}} , \tag{4}$$

where C' is the capacitance per unit length, and C'_0 and Z_{c0} are the capacitance per unit length and characteristic impedance, respectively, when replacing the dielectric substrate by air.

Obtained HBEM results for characteristic impedance will be compared with FEMM software [9], and an error rate calculated as

$$\delta[\%] = \left| \frac{Z_{\text{c}}^{\text{HBEM}} - Z_{\text{c}}^{\text{FEMM}}}{Z_{\text{c}}^{\text{FEMM}}} \right| \cdot 100 , \tag{5}$$

where indexes HBEM and FEMM correspond to the HBEM and FEMM results, respectively.

3. RESULTS AND DISCUSSIONS

The characteristic impedance results convergences of the single and coupled elliptic-shaped microshield lines are given in Fig. 3a and Fig. 3b, respectively.

Dimensions of the single microshield line from Fig. 1a, are:

$\varepsilon_{\text{r}} = 6$, $a/w = 4.0$, $b/w = 3.0$, $d/w = 0.2$ and $h_1/w = h_2/w = 1.0$.

For the coupled structure from Fig. 1b, the parameters are following:

$\varepsilon_{\text{r}} = 6$, $a/w = 4.0$, $b/w = 3.0$, $d/w = 0.2$, $s/w = 0.5$ and $h_1/w = h_2/w = 1.0$.

The good results convergence was achieved already for 1000 unknowns, so that number of unknowns will be used for all following calculations. Additionally, the computation time, indicated by a red dotted line, is displayed. Both figures also include the results obtained through FEMM 4.2 simulation software [9], utilized to validate the computation approach. This software relies on the application of the finite element method.
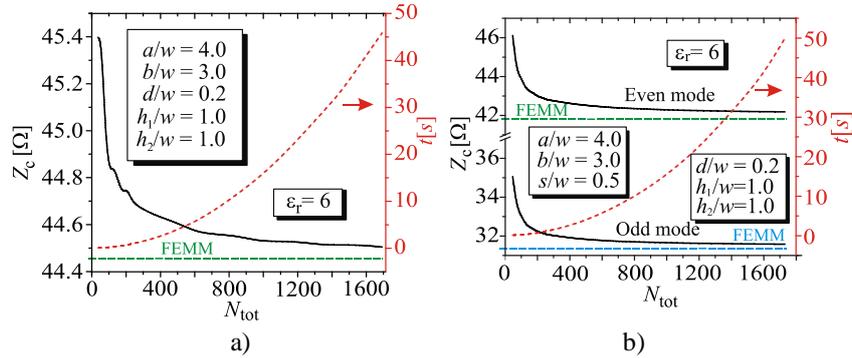
Fig. 3 Results convergence for: a) single and b) coupled (even and odd modes) elliptic-shaped microshield lines

The characteristic impedance values versus strip thickness are shown in Table 1 for the geometry from Fig. 1a. The microshield dimensions are: $\varepsilon_r = 6$, $a / w = 4.0$, $b / w = 3.0$, $h_1 / w = 1.0$ and $h_2 / w = 1.5$. Those results have been compared with the FEMM software results. The error rate, calculated using Eq. (5), is also shown.

Table 1 Characteristic impedance [Ω] versus strip thickness

d / w	HBEM	FEMM	$\delta[\%]$
0.05	53.942	53.466	0.90
0.10	52.010	51.673	0.65
0.15	50.307	50.042	0.53
0.20	48.721	48.510	0.43

Number of finite elements in FEMM application is about 250000. Increasing the strip thickness, the characteristic impedance and effective relative permittivity decrease. Note that the values given in Table 1 are in a very good agreement and the maximum error rate is less than 1%.

Tables 2 and 3 give the characteristic impedance and effective relative permittivity distribution versus normalized microshield width, a / w, for substrate permittivity $\varepsilon_r = 6$ for single and coupled circular-shaped microshield lines. The other parameters are:

$b / w = 3.0$, $d / w = 0.2$, $h_1 / w = 1.0$ and $h_2 / w = 1.5$ (single line) and

$b / w = 3.0$, $d / w = 0.2$, $s / w = 0.5$, $h_1 / w = 1.0$ and $h_2 / w = 1.5$ (coupled line).

Table 2 Characteristic impedance Z_c [Ω] versus microshield width, a / w

	single		coupled (even mode)		coupled (odd mode)	
a / w	HBEM	FEMM	HBEM	FEMM	HBEM	FEMM
3.5	48.670	48.456	45.607	45.507	32.370	32.246
4	48.721	48.501	45.963	45.860	32.548	32.419
4.5	48.740	48.509	46.029	45.926	32.584	32.449
5	48.763	48.512	46.055	45.936	32.604	32.453
6	48.834	48.511	46.035	45.939	32.598	32.454
7	48.804	48.502	46.028	45.936	32.604	32.451
8	48.820	48.498	46.041	45.933	32.622	32.448

Table 3 Effective relative permittivity $\varepsilon_r^{\text{eff}}$ versus microshield width, a/w.

	single		coupled (even mode)		coupled (odd mode)	
a/w	HBEM	FEMM	HBEM	FEMM	HBEM	FEMM
3.5	2.9263	2.9579	3.0314	3.0639	2.9342	2.9715
4	2.9273	2.9610	3.0534	3.0890	2.9477	2.9879
4.5	2.9255	2.9617	3.0563	3.0943	2.9486	2.9915
5	2.9219	2.9617	3.0535	3.0957	2.9452	2.9927
6	2.9113	2.9618	3.0522	3.0959	2.9430	2.9929
7	2.9126	2.9626	3.0484	3.0962	2.9384	2.9932
8	2.9086	2.9626	3.0425	3.0962	2.9320	2.9933

In Tables 2 and 3 the FEMM results [9] are also presented. A good results match is achieved. The characteristic parameters presented in those tables do not change significantly, regardless of the microshield width.

Taking into account that visual changes are easier to notice, the effects of variations in other parameters, for easier analysis, will be shown graphically in the following figures for elliptic and circular-shaped microshield lines.

Fig. 4 gives the characteristic impedance distribution versus normalized substrate thickness h_2/w, for different values of dielectric permittivity ε_r for single (a) and coupled (b) (even and odd modes) elliptic-shaped microshield lines. The odd mode values are denoted with dashed red lines in Fig. 4b.
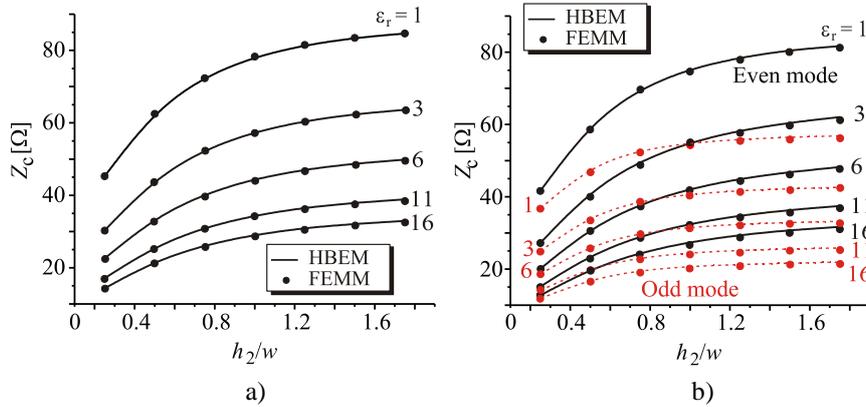

Fig. 4 Characteristic impedance versus h_2/w, (varied ε_r) for: a) single and b) coupled elliptical-shaped microshield lines

The other dimensions are:
$a/w = 4.0$, $b/w = 3.0$, $d/w = 0.2$ and $h_1/w = 1.0$ (single line) and
$a/w = 4.0$, $b/w = 3.0$, $s/w = 0.5$, $d/w = 0.2$ and $h_1/w = 1.0$ (coupled line).

When the substrate permittivity increases, the characteristic impedance decreases. Increasing the substrate thickness, the characteristic impedance increases too. Those changes are smaller if $h_2/w > 1.2$. The characteristic impedance results for the odd mode

are smaller than even mode values. It is interesting to notice that for the certain combinations of parameters the characteristic impedances for both modes can be equal.

The distributions of characteristic impedance are plotted in Fig. 5a and 5b against the normalized microshield high, h_1 / w, for various strip thicknesses, for single (Fig. 5a) and coupled (Fig. 5b) circular-shaped microshield lines. The parameters are:

$\varepsilon_r = 6$, $a / w = 4.0$, $b / w = 3.0$ and $h_2 / w = 1.5$ (single line) and

$\varepsilon_r = 6$, $a / w = 4.0$, $b / w = 3.0$, $s / w = 0.5$ and $h_2 / w = 1.5$ (coupled line).

It can be noticed that increasing the parameter h_1 / w, the characteristic impedance increases too. When the strip thickness increases the characteristic impedance decreases.

An influence of strips thickness on the characteristic impedance values for coupled microshield line is presented in Fig. 5c. The additional parameter is the strips distance. Input parameters are: $\varepsilon_r = 6$, $a / w = 4.0$, $b / w = 3.0$, $h_1 / w = 1.0$ and $h_2 / w = 1.5$.
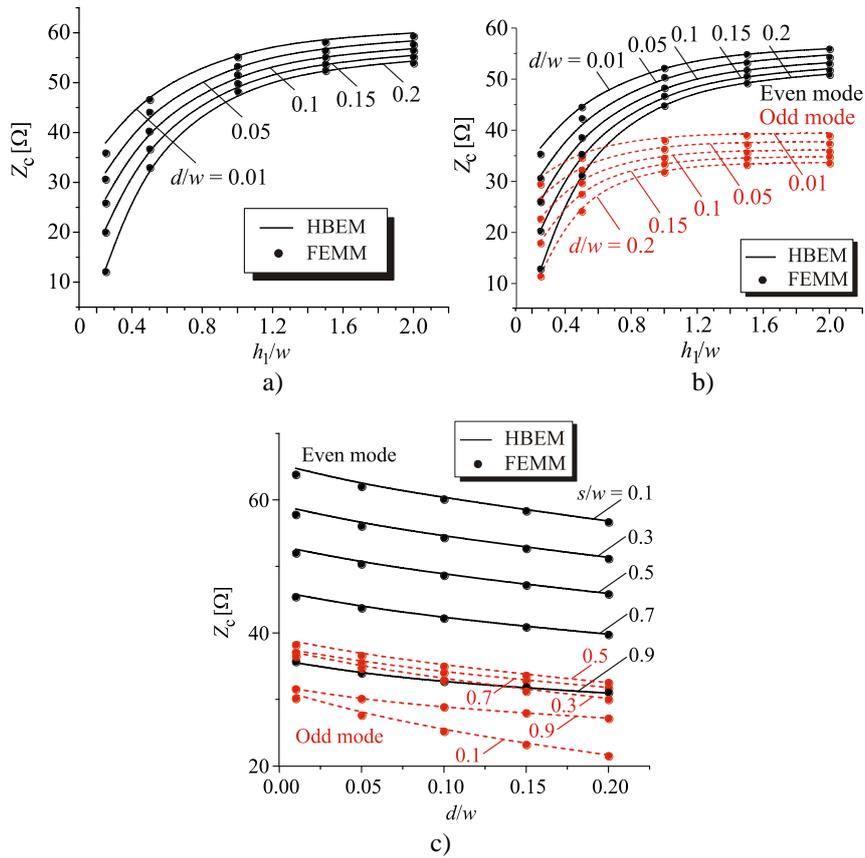

Fig. 5 Characteristic impedance versus: a) h_1 / w (varied d / w) for single circular-shaped microshield line; b) h_1 / w (varied d / w) for coupled circular-shaped microshield line; c) d / w (varied s / w) for coupled microshield line.

Increasing the strips distance, the characteristic impedance of even mode decreases. But, the characteristic impedance in odd mode firstly increases then decreases for $s/w > 0.5$.

It is also interesting to notice that the characteristic impedance values of odd mode, when s/w is 0.3, are approximately equal to the values when the parameter s/w is 0.9 for the even mode, when $d/w > 0.1$.

Equipotential curves for the single as well as coupled microshield lines for different values of h_2/w are given in Fig. 6, for the following parameters:

$\varepsilon_r = 6$, $a/w = 4.0$, $b/w = 3.0$, $d/w = 0.2$ and $h_1/w = 1.0$ (single line) and

$\varepsilon_r = 6$, $a/w = 4.0$, $b/w = 3.0$, $s/w = 0.5$, $d/w = 0.2$ and $h_1/w = 1.0$ (coupled line).

One can observe the effects of the microshield cross-section on potential distribution.
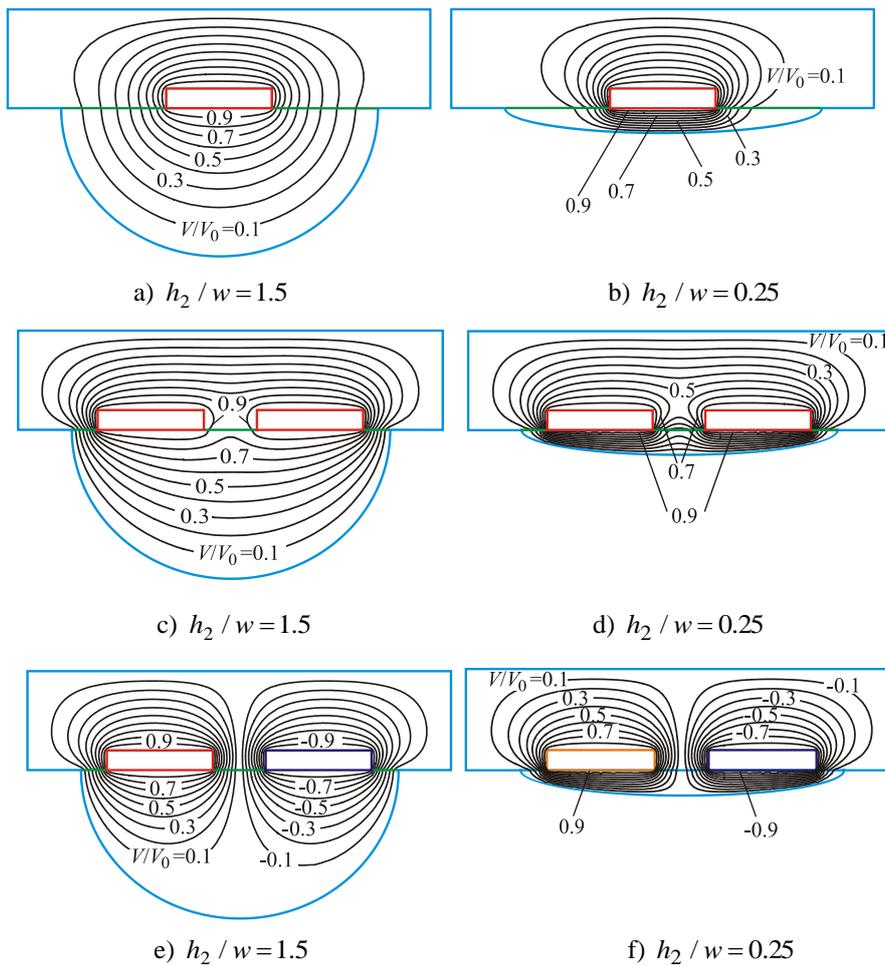

Fig. 6 Equipotential curves distribution for single and coupled microshield lines:
a) and b) single; c) and d) coupled (even mode); e) and f) coupled (odd mode)

3D potential distribution in $x0y$ plane is given in Fig. 7 for the coupled geometries (even and odd modes) shown in Figs. 6c and 6e. Influences of different strips potentials as well as microshield line shape are evident.
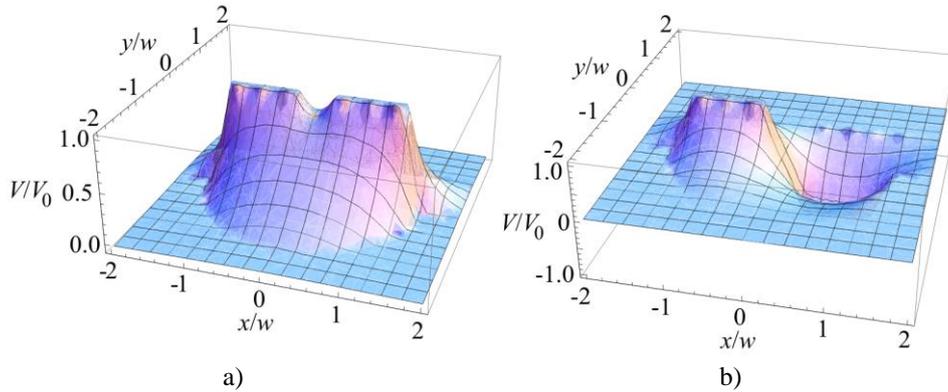

Fig. 7 Normalized potential distribution of a coupled microshield line in $x0y$ plane for:
a) even and b) odd modes

Another comparison can be made between the HBEM results and those given in [7]. The characteristic parameters distribution versus the slot width s and effective relative permittivity is illustrated in Fig. 8 for the single microshield line with elliptical cross-section with the following parameters, taken from [7]: $b = 1385.64$ μm, $h_1 = 3$ mm and $h_2 = 400$ μm and different values of substrate permittivity $\varepsilon_r = 2.55$, 3.78, 10 and 12.9.
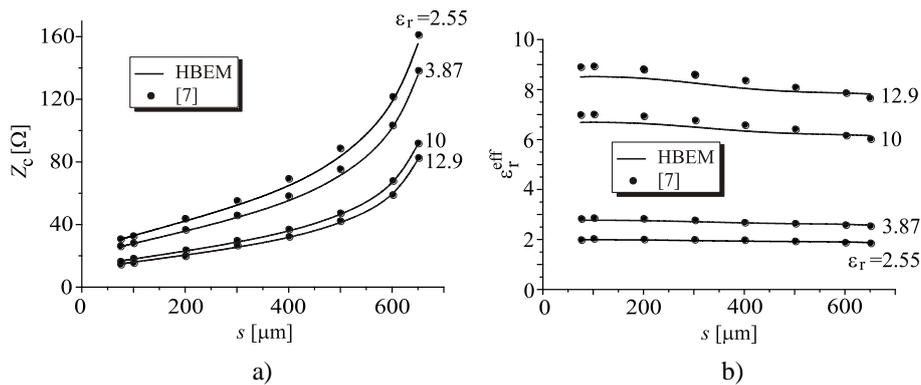

Fig. 8 a) Characteristic impedance and b) effective relative permittivity versus slot width s (varied ε_r) for single elliptic-shaped microshield line

The results from [7] are shown in the same figure. In this comparison some assumptions should be done, because the authors in [7] take into account that the conductor's thickness is negligible and the microshield width (parameter a) is infinite.

Considering that the results given in Tables 2 and 3 show that the characteristic parameters do not change significantly, regardless of the microshield width, the additional parameters

necessary for the HBEM application are $d\,/\,w = 0.02$ and $a\,/\,w$ {4÷60}. Widening the slot leads to higher characteristic impedance and minimal alternations in the effective relative permittivity. Raising the substrate's permittivity results in a decrease in characteristic impedance, as already observed in Fig. 4, while also causing an increase in effective relative permittivity, which can be seen from Fig. 8.

4. CONCLUSION

The characteristic impedance results obtained through the HBEM exhibit a high degree of concurrence with the FEMM outcomes. Demonstration of the impact of microshield dimensions on characteristic parameters has been showcased for both single and coupled structures. This method's efficacy in analysing analogous geometries, valuable in practical applications, has been established.

When employing the HBEM, the main diagonal of the system matrix exhibits the highest values. This characteristic contributes to the improved conditioning of the system of linear equations, resulting in shorter computation time. In formal mathematical representation, the HBEM bears resemblance to the boundary element method (method of moments), yet a crucial disparity lies in both the physical underpinnings and the matrix establishment process. It is important to highlight that, in the application of the HBEM, integration of any form is avoided. In contrast, the method of moments solutions invariably involves numerical integration, thereby introducing challenges in resolving non-elementary integrals. The HBEM simplicity and precision remain evident comparing to the other methods, and as the number of equivalent electrodes increases, a close results match is obtained.

REFERENCES

[1] M. Perić, S. Ilić, N. Ivković and I. Jovanović, "Characteristic parameters determination of circular-shaped microshield lines", In Proceedings of the 16th International Conference on Applied Electromagnetics – *ПEC 2023,* Faculty of Electronic Engineering of Niš, Niš, Serbia, August 28-30, 2023 pp. 150–153.

[2] H. Sun and Y. Wu, "Research on cut-off wavelength of dominant mode and field patterns in trapezoidal microshield lines", *Turkish Journal of Electrical Engineering and Computer Sciences*, vol. 20, no. 4, pp. 463–477, 2012.

[3] J.-F. Kiang, "Characteristic impedance of microshield lines with arbitrary shield cross section", *IEEE Trans. on Microwave Theory and Techniques*, vol. 46, no. 9, pp. 1328–1331, 1998.

[4] N. Yuan, C. Ruan and W. Lin, "Analytical analyses of V, elliptic and circular-shaped microshield transmission lines", *IEEE Trans. on Microwave Theory and Techniques*, vol. 42, no. 5, pp. 855–859, 1994.

[5] N. Dib and L. Katehi, "Impedance calculation for the microshield line", *IEEE Microwave and Guided Wave Letters*, vol. 2, no. 10, pp. 406–408, 1992.

[6] E. Costamagna and A. Fanni, "Conformal mapping analysis of microshield transmission lines", *In Proceedings of ISSE'95 – International Symposium on Signals, Systems and Electronics*, San Francisco, CA, USA, 1995, pp. 463–466.

[7] S. Kaya, M. Turkmen, K. Guney and C. Yildiz, "Neural models for the elliptic- and circular-shaped microshield lines", *Progress in Electromagnetics Research B,* vol. 6, pp. 169–181, 2008.

[8] M. Perić, S. Ilić, A. Vučković and N. Raičević, "Quasi-static TEM analysis of V-shaped microshield lines", In Proceedings of the 15th International Conference on Telecommunication in Modern Satellite, Cable and Broadcasting Services - TELSIKS 2021, Niš, Serbia, October 20−22, 2021, pp. 149−152.
[9] D. Meeker, FEMM, ver. 4.2, available at: http://www.femm.info/wiki/Download.
[10] M. Perić, S. Ilić, S. Aleksić and N. Raičević, "Application of hybrid boundary element method to 2D microstrip lines analysis", *Int. Journal of Applied Electromagnetics and Mechanics*, vol. 42, no. 2, pp. 179–190, 2013.
[11] M. Perić, S. Ilić, S. Aleksić and N. Raičević, "Characteristic parameters determination of different striplines configurations using HBEM", *ACES journal*, vol. 28, no. 9, pp. 858–865, 2013.
[12] M. Perić et al., "Covered microstrip line with ground planes of finite width", *FACTA Universitatis, Series: Electronics and Energetics*, Serbia, vol. 27, no. 4, pp. 589–600, 2014.
[13] M. Perić, S. Ilić, A. Vučković and N. Raičević, "Improving the efficiency of hybrid boundary element method for electrostatic problems solving", *ACES journal*, vol. 35, no. 8, pp. 872–877, 2020.